

Use of Anomalous Scattering in SAXS Measurements

K. D. Finkelstein¹, J. Goodisman², and L. Pollack³

¹Cornell High Energy Synchrotron Source, Cornell University, Ithaca NY

²Syracuse University, Syracuse NY

³Applied & Engineering Physics, Cornell University, Ithaca NY

Introduction

Anomalous (or resonant) scattering refers to changes of the x-ray atomic scattering amplitude when the x-ray energy is near an absorption edge. Small angle x-ray scattering (SAXS) can reveal global, low resolution information on size and shape of electron density variations at colloidal length scales. Anomalous small angle scattering (ASAXS) permits study of one component in a multi-component system [a review is found in Ref. [1]]. In this article we discuss two new applications of ASAXS at CHESS: *in-situ* monitoring of metal catalyst particle size, and probing counter-ion condensation around biological polymers.

Anomalous Scattering: a brief introduction

X-ray scattering from individual atoms in a molecule, solution, or complex depends to first approximation on the spatial distribution of the electron cloud around the nucleus and on the momentum transfer \mathbf{Q} . Near forward scattering ($Q=0$) the scattering amplitude is proportional to the number of electrons in the cloud. For example when rubidium (atomic number $Z = 37$) has valence +1 in solution, the x-ray scattering factor is $Z - 1 = 36$ electrons/atom. However, if the incident energy is tuned near the rubidium K-edge (15.2 keV) the atom is resonantly excited and the scattering amplitude is reduced. Figure 1 shows the magnitude of this reduction under experimental conditions using a double bounce Si(111) monochromator at C1. The upper curve is f'' , the imaginary component of anomalous scattering, obtained by measuring normalized transmission through a solution. The lower curve is f' , the real part of anomalous scattering, obtained by Kramers-Kronig transformation of f'' using the program CHOOCH [2].

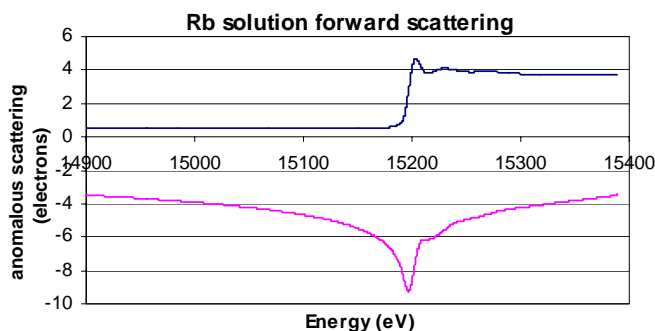


Fig 1: Real (bottom), imaginary (top) anomalous scattering (in classical electron units) plotted against x-ray energy for rubidium ions in solution near the K-edge. Subtraction of SAXS patterns taken at two x-ray energies below the K-edge can be used to measure the signal from Rb ions.

ASAXS is done by measuring two scattering patterns, one with x-ray energy just below the absorption edge where f' is negative and f'' is very small, and at a second energy several hundred eV below the edge. The anomalous difference in the real part of scattering from atoms of interest, $\Delta f'$ is typically 2 to 5 electrons at K-edges, and up to 10 electrons at L-edges.

To extract information on the spatial distribution of anomalous scattering ions, we collect 4 patterns (signal and background scattering at each energy), and measure the incident and sample transmitted intensity at these energies.

The CHESS C1 station is well suited for ASAXS because it has a long flight path, is compatible with CCD area detectors, and users have a choice of tunable x-ray monochromators that deliver high flux on small specimens. Two monochromators used for this work are: a vertical double bounce sagittal focusing mono for precise energy scanning (beam path indicated by dashed line in Figure 2), and a horizontal focus side-bounce mono with simultaneous dual energy capability for time dependent studies.

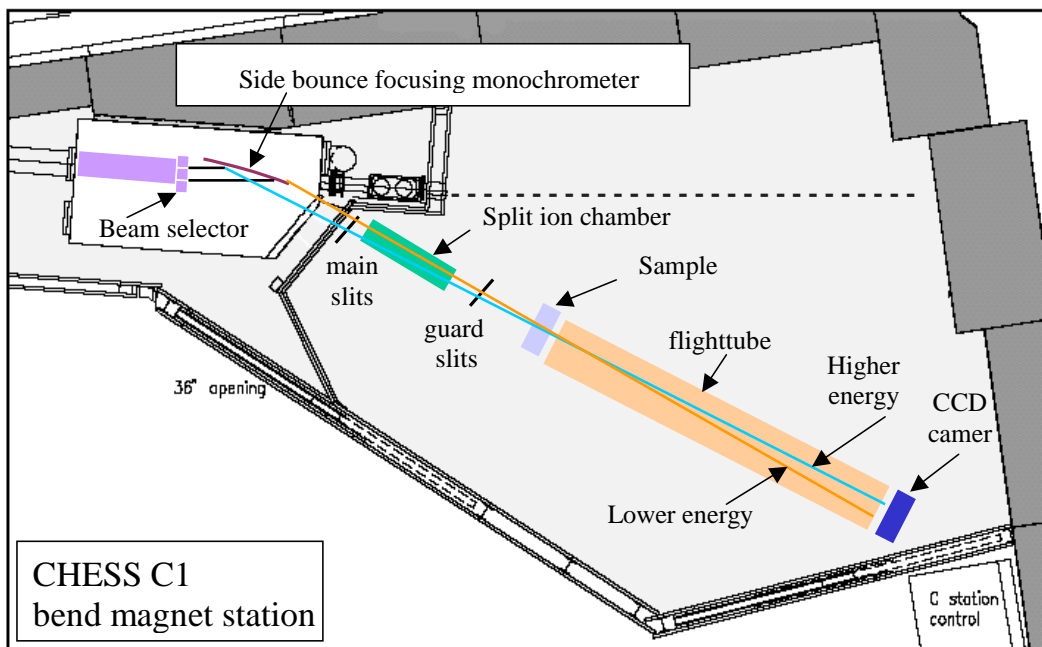


Fig 2: CHES C1 station has x-ray beams from several monochromators. A side bounce mono deflects beam horizontally to produce a mono- or polychromatic focus (two colors). The double bounce mono for energy scanning (dashed line) gives focused or unfocused radiation from 6 to about 30 KeV.

Examples:

1) Simultaneous dual-energy ASAXS

Mordenite is a zeolite mineral with a very large internal surface area composed of channels up to 14Å in diameter. Zeolite is a catalytic support into which metal (in this case platinum) can be incorporated by ion exchange. When mordenite is heated in a controlled atmosphere the metal atoms agglomerate into small particles trapped in the channels. If metal particles are randomly distributed in this structure, ASAXS at the platinum L-absorption edge can be used to measure the distribution of particle sizes.

H. Brumberger and co-workers used dual-energy ASAXS to study how particle size depends on heating rate, temperature, and gas atmosphere during particle formation. To follow the time evolution of particle growth, we used slits upstream of a sidebounce mono to select two rays (two energies) incident on the sample. These beams diverge to form SAXS patterns displaced from one another on a CCD detector one meter downstream of the sample. Beam intensity transmitted through the sample is monitored by diodes located in beamstops just upstream of the detector. A series of patterns were recorded at ½ minute time intervals, over several hours during sintering.

In Figure 3 x-ray scattering during an extended sample heating cycle is displayed in Porod form. If the material is composed of regions of constant electron density separated by sharp boundaries

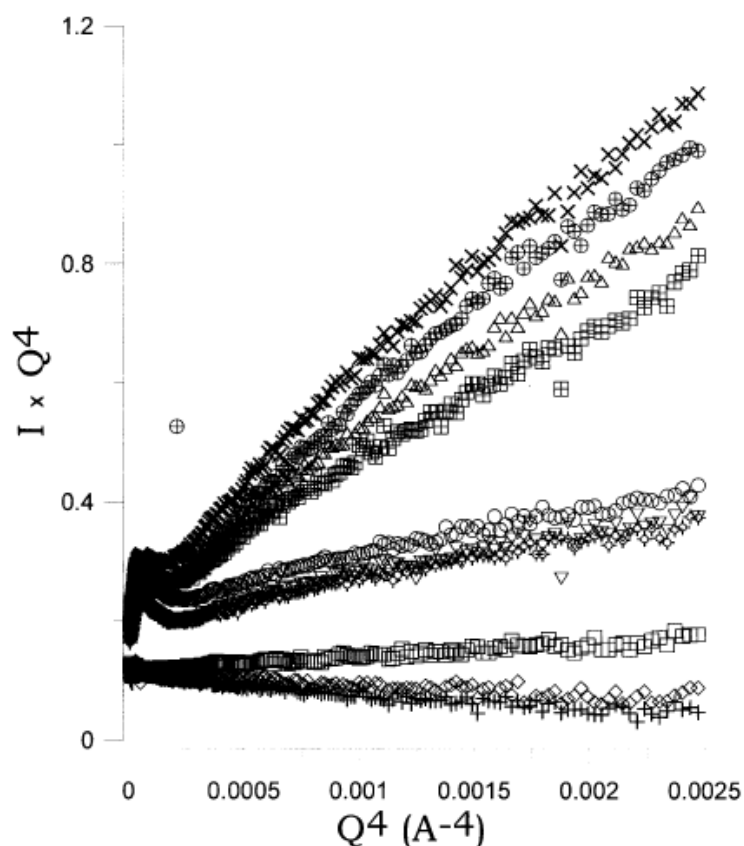


Fig 3: Porod plots ($Q^4 \cdot \text{Intensity}$ vs. Q^4) of the radial difference in SAXS at two wavelengths. Intensity is normalized to account for sample transmission. The intensity rises with time in this sequence of measurements spanning about 2 hours and three sample conditions: the weakest scattering (3 lower curves) corresponds to temperature below 400C and helium atmosphere, the middle curves were obtained at 400C and atmosphere 10% oxygen/90% helium, the last group (4 curves displaying rapidly increasing slope) were collected in a reducing atmosphere (pure H2). The increase of intensity at large Q is an indication that small particles are being formed.

[3], $I(Q) \cdot Q^4$ versus Q^4 approaches a constant at large Q ; where the constant is a measure of total surface area on the boundary. A generalized Porod form [$Q^4 I(Q) = k + pQ^4$] is used to account for atomic scale fluctuations (fuzzy boundaries)[4]. Our data do not display Porod behavior at large Q so we have modeled the scattering using a particle size distribution function with parameters adjusted to fit the data over the measured Q -range [5]. When applied over the full time course of catalyst preparation this analysis gives a surprising result; it suggests mean platinum particle size actually *decreases* as sintering progresses.

Qualitatively, the particle growth behavior is visible at low angles, $Q^4 < 0.0003$ ($Q \leq 0.125 \text{ \AA}^{-1}$), in Figure 3. During initial heating (the lowest curves where temperature is below 250C) the difference scattering is flat and weak suggesting the platinum is uniformly distributed throughout the zeolyte. The next group of curves, the middle group on the vertical axis, collected between 250 and 400C, show a peak at $Q_0 \approx 0.08 \text{ \AA}^{-1}$ corresponding to an upper limit on particle size set by cage size ($1/Q_0 \sim 12 \text{ \AA}$). The third group highest on the vertical axis, were collected when sample temperature was stabilized at 400C. They show additional scattering out to $Q = 0.125 \text{ \AA}^{-1}$ ($1/Q_0 \sim 8 \text{ \AA}$). This is consistent with small particles forming between larger ones; the mean particle size actually shrinks as sintering progresses.

A large platinum surface area (many small particles) is critical to catalytic activity. Measurements that quantitatively connect size distribution to process conditions are an essential tool in designing highly efficient industrial catalysts.

These experiments were carried out by H. Brumberger (deceased), D. Hagrman, and K. Finkelstein, and the analysis was completed by J. Goodisman. The work was supported by a grant from The Petroleum Research Fund.

2) A biological application

Figure 4 shows an atomic scale model of (negatively charged) DNA surrounded by positively charged (or counter-) ions, shown in blue. Negatively charged (co-) ions are shown as green spheres.

Ions in solution are attracted to the highly charged strands that compose biopolymers such as DNA and proteins. The interaction of ions with these charged molecules is biologically important and strongly affects biomolecular conformation as in RNA folding or DNA condensation. Although it has been recognized for many years that ions contribute to SAXS profiles of ion-DNA solutions, recent experiments using ASAXS at C1 have measured signals that report directly on the spatial distribution of ions around the nucleic acid strand (Figure 4).

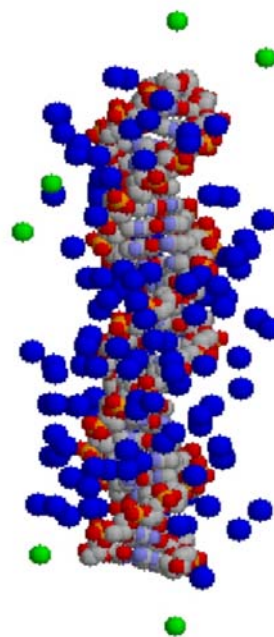


Fig 4: An atomic scale model of (negatively charged) DNA surrounded by positively charged (or counter-) ions, shown in blue. Negatively charged (co-) ions are shown as green spheres

Theories describing the arrangement of oppositely charged (or counter-) ions around DNA have appeared in the literature since the 1970's [6]. However, experimental verification of these theories has proved challenging. Simple theories, based for example on mean field approximations (e.g. the Poisson Boltzmann equation) do not predict the dramatic influence of counterions on biomolecules. A most important example is the attraction between like-charged strands that is a signature of both protein and nucleic acid systems [7]. The physical origin of this biologically critical interaction in DNA has yet to be elucidated.

To address these issues, we applied ASAXS to probe the distribution of ions around short DNA strands in solution [8], working at x-ray energies near counterion absorption edges. To probe the distribution of monovalent ions, we examined Rb-DNA (Rb K-edge is at 15.2 keV); to probe the distribution of divalent counterions we examine Sr-DNA (Sr K-edge is at 16.1 keV). In contrast with the previous application there is no time dependence and the samples scatter relatively weakly so a focused double bounce mono is used and for each ion scattering profiles are acquired at two energies in sequence. Raw scattering profiles shown in Figure 5 correspond to one Rb-DNA sample at two energies. The normalized difference (anomalous) curve, a small fraction of the total scattering, is shown in black.

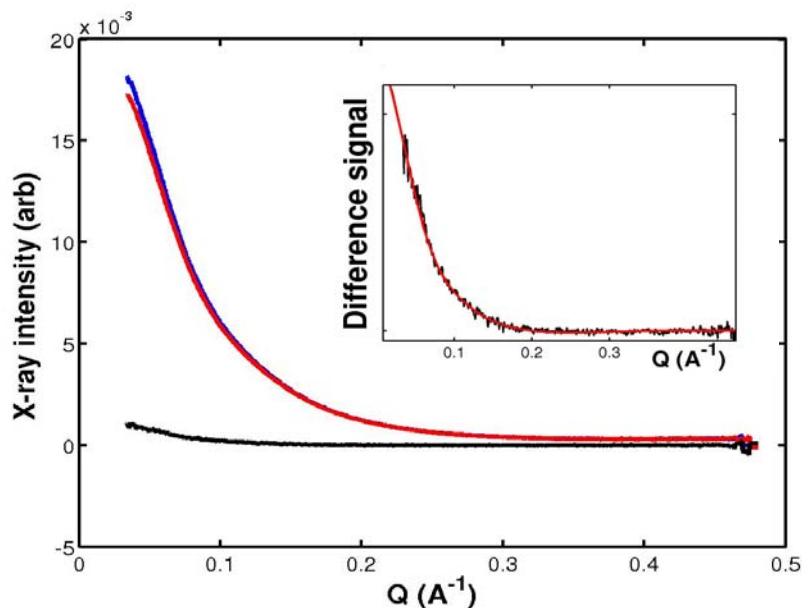


Fig 5: This figure shows raw scattering profiles for Rb-DNA. Rubidium concentration for these experiments is 0.1M, and DNA concentration is 0.2 mM. The blue curve is raw data acquired at x-ray energy well below the rubidium edge. The red curve is a scattering profile acquired just below the edge, adjusted for fluorescence. The shape of the difference curve, black, reflects the spatial distribution of Rb^+ counterions. The inset shows on expanded scale a fit to the difference signal that employs an ion distribution calculated from the non-linear Poisson Boltzmann equation [details are in Ref. 8].

To analyze the data, we begin with predictions of real space distributions for the ions and the DNA. Scattering profiles are calculated using these ideal distributions and are compared with our measurements. Good agreement between the two is a validation of the theoretical assumption, in this case the distribution of counterions. These experiments find good agreement between measurements of monovalent and divalent ion distributions around DNA and theoretical predictions based on the non-linear Poisson-Boltzmann model [8].

Our goal in future experiments is to push the system into more highly charged regimes where deviations from mean field theory dominate behavior. These experiments seek to: a) identify the limiting conditions under which this simpler theory applies, and b) study physical effects resulting from strong correlations between counterions.

This work was carried out in collaboration with R. Das, T.T. Mills, L.W. Kwok, G.S. Maskel, I.S. Millett, S. Doniach, D. Herschlag, K. Andresen, H. Y. Park, H. Smith and J.S. Lamb. This project was supported by NASA, the NIH and the NSF, through Cornell's NBTC.

References:

- [1] A. Naudon, "Anomalous Small Angle X-ray Scattering", in *Modern Aspects of Small-angle Scattering*, H. Brumberger, Editor. Kluwer Academic Publishers: Dordrecht/Boston/London (1993).
- [2] G. Evans and R. F. Pettifer, *J. Appl. Cryst.* **34**, 82-86 (2001).
- [3] O. Glatter & O. Kratky, "Small-angle X-ray Scattering", Academic Press, New York (1982).
- [4] H. Brumberger, J. Goodisman, R. Ramaya, S. Ciccariello, *J. Appl. Cryst.* p. 526 (1996).
- [5] H. Brumberger, D. Hagrman, J. Goodisman, K.D. Finkelstein, "In-Situ Anomalous SAXS From Metal Particles in Supported-Metal Catalysts", submitted to *J. Applied Crystallography* (2003).
- [6] C.F. Anderson and M.T. Record, *Annual Review of Biophysics and Biophysical Chemistry*, **19**: p. 423-465 (1990).
- [7] A.Y. Grosberg, T.T. Nguyen, and B.I. Shklovskii, *Reviews of Modern Physics*, **74(2)**: p. 329-345 (2002).
- [8] R. Das, Mills, T.T., Kwok, L.W., Maskel, G.S., Millett, I.S., Doniach, S., Finkelstein, K.D., Herschlag, D., Pollack, L., *Phys. Rev. Lett.*, **90**: p. 188-203 (2003).